Figure 5. Plot of the number of CO molecules dissociated per potassium atom as a function of potassium coverage.

by the dissociation of adsorbed CO. The extent to which scrambling of the isotopically labeled CO molecule occurs depends on both K coverage and CO exposure.

The plot of the fraction of CO dissociated as a function of K coverage (Figure 3) demonstrates that the effect of the alkali on the number of molecules dissociating is very pronounced. Over 80% of the adsorbed CO dissociates at $\Theta_K = 0.15$. Using the CO saturation coverage of $\Theta_{CO} = 0.75$ for the clean Rh(111) surface made it possible to determine the number of CO molecules which dissociate per adsorbed K atom. Such a curve is plotted in Figure 5 as a function of K coverage. Up to three CO molecules dissociate per coadsorbed potassium atom at a coverage $\Theta_K = 0.1$, a very marked effect indeed. The curve rapidly attains a maximum, followed by a gradual decrease. This suggests that (1) a critical potassium coverage (i.e., potassium separation) is needed to induce CO dissociation, and (2) site blocking by potassium at higher coverages limits CO adsorption. This results in the ratio CO_{diss}/K decreasing slowly as the potassium coverage increases. These competitive effects result in a peak maximum. Recent calculations by Norskov et al.[7] suggest that sites adjacent to the alkali should be very strongly affected by the alkali, whereas the second nearest neighbors experience a much reduced effect. These results are consistent with our data since the number of CO molecules that dissociate is that which would be expected to pack adjacent to an isolated K atom.

Results on CO coadsorption with Na on Ru[8] suggest that the alkali is well dispersed on the surface at all coverages, thus

(7) Norskov, J. K.; Holloway, S.; Lang, N. D. *Surf. Sci.* **1984**, *137*, 65.
(8) Doring, E. L.; Semancik, S. *Surf. Sci.* **1983**, *129*, 177.

permitting access of several carbon monoxide molecules to each alkali atom.

The simultaneous desorption of CO and K in the high-temperature state as shown in Figure 1 indicates that potassium and either C or O (or both) are associated with one another and that the rate-limiting step is the decomposition of this surface complex.

Measurement of the scrambling parameter yields a value of p considerably larger than that expected for molecular desorption, confirming that the highest temperature states are indeed due to dissociated CO. The behavior as a function of CO exposure can be explained by assuming that isolated C or O atoms (or both species) have some mobility on the Rh(111) surface. At low CO coverages (Figure 4a) the C and O adatoms from different molecules are sufficiently remote from each other that the probability of scrambling is small. As the coverage increases, the fragments from different molecules come into closer proximity and can then scramble. At even higher coverages the atoms become less mobile, either since they are close packed or because they are associated with potassium and are thus immobilized, inhibiting significant scrambling.

Finally, it should be emphasized that EEL spectroscopy shows no evidence that potassium causes CO to dissociate on the Rh(111) surface[1] since no C–metal or O–metal vibrations are observed. TPD evidence clearly indicates that CO does indeed dissociate on a potassium predosed surface, and the absence of any EELS evidence of dissociated CO on the surface may be suggestive that the dissociation (and scrambling) and desorption occur as a concerted process.

Conclusion

The coadsorption of potassium with CO on Rh(111) induces dramatic changes in the chemisorption properties of CO. Isotopic mixing measurements verify that CO dissociation occurs with coadsorbed potassium ($\Theta_K > 0.10$) but does not occur on the potassium-free Rh(111) surface. The simultaneous desorption of potassium and CO for the dissociated state indicates that direct interactions are responsible for CO dissociation and that up to three CO molecules are dissociated per potassium atom.

Registry No. K, 7440-09-7; CO, 630-08-0; Rh, 7440-16-6.

Noncontinuum Solvent Effects upon the Intrinsic Free-Energy Barrier for Electron-Transfer Reactions

Joseph T. Hupp and Michael J. Weaver*

Department of Chemistry, Purdue University, West Lafayette, Indiana 47907 (Received: August 13, 1984)

A phenomenological electrochemical approach is outlined by which "noncontinuum" contributions to the outer-shell intrinsic barrier to electron transfer, ΔG^*_{os}, resulting from specific reactant–solvent interactions can be estimated from the measured dependence of the formal potential upon the molecular and structural properties of the solvent. A simplified derivation, based on electrochemical half-reactions, of the conventional dielectric continuum expression is given in order to clarify the physical origins of the outer-shell intrinsic barrier and to identify likely additional noncontinuum components. Numerical calculations for ammine and other redox couples involving specific ligand–solvent interactions indicate that the noncontinuum contributions to ΔG^*_{os} for both homogeneous and electrochemical exchange reactions can be surprisingly small (typically $\lesssim 1$–2 kcal mol^{-1}) even when the thermodynamics of ion solvation are in severe disagreement with the dielectric continuum (Born) predictions. An additional noncontinuum component associated with vibrational distortions of outer-shell solvent may be significant for multicharged aquo complexes and other reactants engaging in strong ligand–solvent hydrogen bonding.

In recent years a number of theoretical approaches have been developed in order to describe the kinetics of outer-sphere electron-transfer processes.[1] It is useful to divide the overall free energy of activation into so-called "intrinsic" and "thermodynamic"

contributions,[2] the former being the component that remains in the absence of the free-energy driving force $\Delta G°$. Since evaluation of the latter component of the activation barrier is relatively straightforward given a knowledge of $\Delta G°$, theoretical efforts have focused attention on methods for calculating the former. These usually treat the intrinsic activation barrier in terms of separate contributions from the intramolecular reorganization of the reactant (inner-shell barrier) and the polarization of the surrounding noncoordinated solvent (outer-shell barrier). Treatment of the former has reached a high degree of sophistication, aided by the acquisition of accurate structural and vibrational data which enable the molecular distortions of the reactant to be calculated quantitatively for a number of reactions.[3] On the other hand, relatively little is known of the molecular structural details associated with outer-shell solvent reorganization. Consequently, this component is usually treated in terms of a model which regards the surrounding solvent as a dielectric continuum.[4]

Until recently, tests of these theoretical treatments were restricted chiefly to "relative rate" comparisons in a given solvent, usually water. These involve comparisons between the rate parameters of closely related reactions, especially between homogeneous self-exchange and cross reactions[5] and with corresponding electrochemical processes,[6] as well as the dependence of rates upon the thermodynamic driving force.[7] Unfortunately, the predicted form of such comparisons are insensitive to the model used for the outer- as well as the inner-shell barrier. Greater insight into the nature of the outer-shell barrier can be obtained by examining the kinetics of suitable homogeneous self-exchange and electrochemical exchange reactions as a function of the solvent. A number of examinations of this type have been reported recently;[8-16] some indicate significant discrepancies with the solvent dependence predicted from the conventional dielectric continuum treatment.

The emergence of quantitative inner-shell structural data along with further theoretical developments has recently spawned several other confrontations between theory and experiment, involving the calculations of rate parameters for individual electron-transfer reactions ("absolute rate" comparisons). These involve scrutiny of homogeneous cross reactions[17,18] and electrochemical pro-

cesses[15,16,18] as well as homogeneous self-exchange reactions.[3,17,18,19] Although reasonable agreement between theory and experiment is obtained under some conditions,[2,3,16,17] significant discrepancies occur in a number of cases.[3,15,18]

The theoretically derived rate constants are commonly larger than the experimental values.[3,15,18] One possible explanation is that the dielectric continuum model used in these calculations underestimates the solvent reorganization barrier. This notion would seem reasonable given that there is extensive evidence that electron transfer is often accompanied by large alterations in the short-range solvent structure, especially for multicharged transition-metal systems which can exhibit strong interactions between the coordinated ligands and the surrounding solvent.[20-23] However, discussions of the likely limitations of the dielectric continuum approach have often been confused by a lack of understanding of the physical origins of nonequilibrium solvent polarization.

We have recently outlined a modification to the dielectric continuum approach by which the intrinsic entropic barrier, ΔS^*_{int} (i.e., the activation entropy that remains in the absence of an entropic driving force), can be calculated from thermodynamic data, thereby circumventing some features of the conventional approach.[24] This utilizes experimental entropy changes measured for the constituent electrochemical reaction(s) (i.e., the "reaction entropies"), $\Delta S°_{rc}$[20]). Larger and more structure-sensitive values of ΔS^*_{int} are obtained than obtained when the conventional dielectric continuum formula is used.[24] In the present paper we describe a related approach by which the influence of short-range reactant–solvent interactions (i.e., "noncontinuum electrostatic" interactions) upon the intrinsic free-energy barrier, ΔG^*_{int}, can be estimated from an analysis of electrochemical thermodynamic data. Besides clarifying the physical origins of solvation effects upon the intrinsic barrier, these considerations provide insight into the extent to which ΔG^*_{int} is likely to differ from the predictions of the conventional continuum model of ionic solvation.

Origin of the Outer-Shell Intrinsic Barrier

Before discussing noncontinuum effects it is useful to clarify the physical origin of the intrinsic free-energy barrier associated with outer-shell solvent reorganization, ΔG^*_{os}, on the basis of the dielectric continuum model. An enlightening mathematical derivation has been given by Marcus.[25] A simplified version of this analysis will first be summarized since it provides a useful framework for incorporating noncontinuum factors.

As for the corresponding treatment of intrinsic entropic barriers,[24] it is useful to consider the energetics of homogeneous electron-transfer processes in terms of a combination of the appropriate pair of electrochemical "half-reactions" having the general form

$$Ox + e^-(\phi_m) \rightleftharpoons Red \tag{1}$$
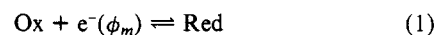
where ϕ_m is the (Galvani) electrode–solution potential difference. For simplicity, we shall initially consider a single such electrochemical reaction in the so-called "weak overlap" limit, where the transition-state stability is unaffected by the presence of the electrode. This approach enables a simple physical picture to be provided of the activation process.[24]

According to the dielectric continuum treatment, the formation of the transition state involves a nonequilibrium solvent polarization process associated with random spatial fluctuations of nearby solvent molecules. This can usefully be perceived in terms of a hypothetical two-step charging process.[25] First, the charge of the

(1) For recent reviews, see: (a) Schmidt, P. P. "Electrochemistry – A Specialist Periodical Report"; Chemical Society: London, 1975; Vol. 5, Chapter 2. (b) Ulstrup, J. "Charge Transfer Processes in Condensed Media"; Springer-Verlag: West Berlin, 1979. (c) Cannon, R. D. "Electron Transfer Reactions"; Butterworths: London, 1980. (d) Dogonadze, R. R.; Kuznetsov, A. M.; Mariagishivili, T. A. *Electrochim. Acta* **1980**, *25*, 1. (e) Sutin, N. *Prog. Inorg. Chem.* **1983**, *30*, 441.

(2) Marcus, R. A. *J. Phys. Chem.* **1968**, *72*, 891. Sutin, N. *Acc. Chem. Res.* **1968**, *1*, 225.

(3) (a) Brunschwig, B. S.; Logan, J.; Newton, M. D.; Sutin, N. *J. Am. Chem. Soc.* **1980**, *102*, 5798. (b) Brunschwig, B. S.; Creutz, C.; McCartney, D. H.; Sham, T.-K.; Sutin, N. *Discuss. Faraday Soc.* **1982**, *74*, 113.

(4) (a) Marcus, R. A. *J. Chem. Phys.* **1965**, *43*, 679. (b) For a recent critical review, see: German, E. D.; Kuznetsov, A. M. *Electrochim. Acta* **1981**, *26*, 1595.

(5) See, for example: (a) Chou, M.; Creutz, C.; Sutin, N. *J. Am. Chem. Soc.* **1977**, *99*, 5615. (b) Marcus, R. A.; Sutin, N. *Inorg. Chem.* **1975**, *14*, 213. (c) Weaver, M. J.; Yee, E. L. *Inorg. Chem.* **1980**, *19*, 1936.

(6) Weaver, M. J. *J. Phys. Chem.* **1980**, *84*, 568.

(7) See, for example: Weaver, M. J.; Hupp, J. T. *ACS Symp. Ser.* **1982**, *198*, 181.

(8) Yang, E. S.; Chan, M.-S.; Wahl, A. C. *J. Phys. Chem.* **1980**, *84*, 3094.

(9) Chan, M.-S.; Wahl, A. C. *J. Phys. Chem.* **1975**, *82*, 2542.

(10) Chan, M.-S.; Wahl, A. C. *J. Phys. Chem.* **1982**, *86*, 126.

(11) Li, T. T.-T.; Weaver, M. J.; Brubaker, Jr., C. H. *J. Am. Chem. Soc.* **1982**, *104*, 2381.

(12) Fawcett, W. R.; Jaworski, J. S. *J. Phys. Chem.* **1983**, *87*, 2972.

(13) Sahami, S.; Weaver, M. J. *J. Electroanal. Chem.* **1981**, *124*, 35.

(14) Weaver, M. J.; Tyma, P. D.; Nettles, S. M. *J. Electroanal. Chem.* **1981**, *114*, 53.

(15) Hupp, J. T.; Liu, H. Y.; Farmer, J. K.; Gennett, T.; Weaver, M. J. *J. Electroanal. Chem.* **1984**, *168*, 313. Farmer, J. K.; Gennett, T.; Weaver, M. J. *J. Electroanal. Chem.*, in press.

(16) (a) Milner, D.; Weaver, M. J.; Gennett, T. *Chem. Phys. Lett.* **1985**, *113*, 213. (b) Gennett, T.; Weaver, M. J. *J. Phys. Chem.*, in press.

(17) Siders, P.; Marcus, R. A. *J. Am. Chem. Soc.* **1981**, *103*, 741.

(18) Hupp, J. T.; Weaver, M. J. *J. Phys. Chem.*, in press. Hupp, J. T. Ph.D. Dissertation, Michigan State University, 1983.

(19) Endicott, J. F.; Kumar, K.; Tamasami, T.; Rotzinger, F. P. *Prog. Inorg. Chem.* **1983**, *30*, 141.

(20) Yee, E. L.; Cave, R. J.; Guyer, K. L.; Tyma, P. D.; Weaver, M. J. *J. Am. Chem. Soc.* **1979**, *101*, 1131.

(21) Weaver, M. J.; Nettles, S. M. *Inorg. Chem.* **1980**, *19*, 1641.

(22) Sahami, S.; Weaver, M. J. *J. Electroanal. Chem.* **1981**, *122*, 155, 171.

(23) Hupp, J. T.; Weaver, M. J. *Inorg. Chem.* **1984**, *23*, 3639.

(24) Hupp, J. T.; Weaver, M. J. *J. Phys. Chem.* **1984**, *88*, 1860.

(25) Marcus, R. A. In "Special Topics in Electrochemistry"; Rock, P. A., Ed.; Elsevier: New York, 1977; also see ref 1a.

reactant Ox is slowly adjusted to an appropriate value, usually about midway between that of the reactant and product, so that the solvent is polarized to an extent identical with that for the transition state (step 1). Then the charge is readjusted to that of the reactant sufficiently rapidly so that the solvent orientation remains unaltered (step 2), thereby yielding the nonequilibrium solvent polarization appropriate to the transition state.

In terms of the equilibrium dielectric continuum model due to Born, the change in free energy associated with charging (or discharging) spherical Ox to form Red in a given dielectric medium, $\Delta G°_{rc,os}$, can be expressed as[26]

$$\Delta G°_{rc,os} = \frac{(Z_{red}^2 - Z_{ox}^2)Ne^2}{2r\epsilon_s} \quad (2)$$

where Z_{ox} and Z_{red} are the ionic charge numbers of Ox and Red, N is the Avogadro number, e is the electronic charge, r is the reactant radius, and ϵ_s is the static dielectric constant of the surrounding solvent medium. Since step 1 involves slow (reversible) charging via a series of thermodynamic states, eq 2 can in principle also describe this process, yielding outer-shell free energies, $\Delta G°_{os}$, corresponding to a series of nonintegral charges between Z_{ox} and Z_{red}. Thus we can write

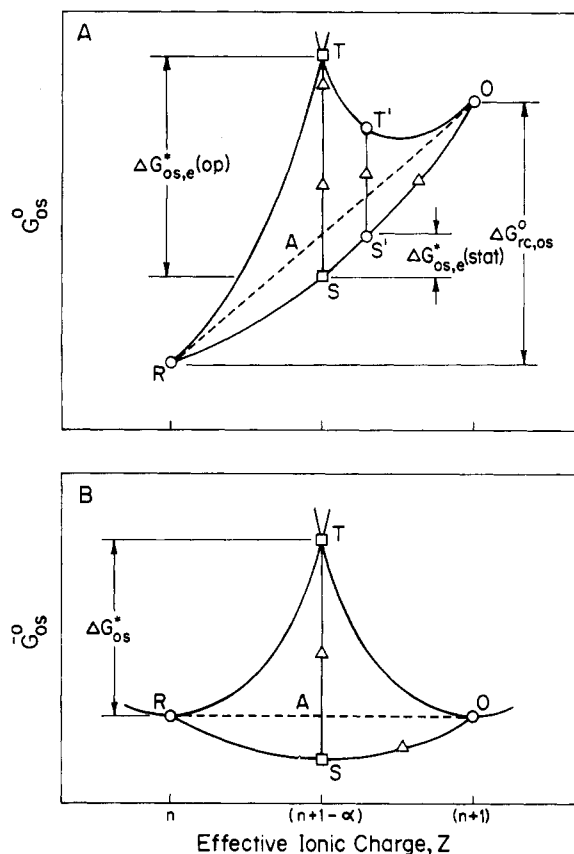$$\Delta G°_{os} = \frac{[(n + 1 - \alpha)^2 - (n + 1)^2]Ne^2}{2r\epsilon_s} \quad (3)$$

where n now represents the charge number in the reduced state, and α represents the fractional charge transferred, starting from the oxidized state having a charge number $(n + 1)$. A resulting plot of the outer-shell free energy, $\Delta G°_{os}$, against the effective ionic charge Z [$=(n + 1) - \alpha$] is shown schematically in Figure 1A (curve OSR, where O represents the oxidized and R the reduced species).

It is important to recognize that the overall intrinsic barrier for the electrochemical reaction 1 refers to a particular potential, $\phi°_m$ (the "standard" or "formal" potential). At this point the difference in free energy between Ox and Red, $\Delta G°_{rc}$, is cancelled by the electron free energy $F\phi°_m$ (i.e., the energy gained by the transferring electron), so that the overall "electrochemical" free energy driving force, $\Delta \bar{G}°_{rc}$, equals zero. A portion of this electron free energy, $F\phi°_{m,os}$, can be considered to be associated with the outer-shell component of $\Delta G°_{rc}$, $\Delta G°_{rc,os}$, such that[27]

$$\Delta G°_{rc,os} = -F\phi°_{m,os} \quad (4)$$

The changes in "chemical" free energy, $\Delta G°_{os}$, anticipated from eq 3 during the step 1 charging process are therefore offset by corresponding changes in the electron free energy, $-\alpha F\phi°_{m,os}$. However, compensation of these two components of $\Delta \bar{G}°_{rc}$ will only be exact when $\alpha = 1$ since the solvational and electrical portions are quadratically and linearly dependent, and respectively, upon the ionic charge. Consequently the plot of the electrochemical free energy $\bar{G}°_{rc,os}$ against the effective ionic charges, shown as curve OSR in Figure 1B, has a symmetrical "bowed" shape. The magnitude of this nonlinearity, i.e., the vertical displacement of the OSR solid curve from the OR dashed straight line (Figure 1A,B), depends on the extent of noncancellation of the opposing solvational and electronic contributions to the energetics of step 1. The resulting "static" contribution to the

(26) Note that the coefficient $1/\epsilon$ appears in eq 2 rather than $(1 - 1/\epsilon_s)$ which is found in the conventional Born expression for the solvation free energy of a given ion. This is because eq 2 is concerned with the difference in the *absolute* electrostatic free energies of the reduced and oxidized forms. Rather than selecting vacuum (where $\epsilon_s = 1$) as the "reference state" as in the Born expression, it is therefore appropriate to formally refer the $\Delta G°_{rc,os}$ values to a hypothetical medium where $\epsilon_s \rightarrow \infty$, for which necessarily $\Delta G°_{rc,os} = 0$; i.e., where the influence of the additional electron in the reduced vs. the oxidized species upon the ion–solvent interactions is entirely nullified by the surrounding solvent dipoles.

(27) The overall magnitude of $\Delta G°_{rc}$ is determined by an inner-shell component as well as the outer-shell term, $\Delta G°_{rc,os}$, considered here. The former arises from the differences in electronic structure between Ox and Red associated with ligand-field stabilization, etc. and is considered to be unaffected by the ion–solvent interactions.


Figure 1. Schematic plots outlining outer-shell free energy–reaction coordinate profiles for redox couples $O + e^- \rightleftharpoons R$ on the basis of the hypothetical two-step charging process, as outlined in the text. (A) Y axis: ionic free energy; (B) Y axis: electrochemical free energy (i.e., including energy of reacting electron). The pathways OT′S′ and OTS, marked by arrows, represent hypothetical two-step charging process, starting from the stable oxidized form, by which the nonequilibrium free-energy profile OT′T corresponding to the thermal activation process can be deduced. T is the transition state since this forms the intersection point of the two nonequilibrium free-energy curves starting from the oxidized and reduced forms, OT and RT, respectively.

outer-shell intrinsic barrier, $\Delta G°_{os,e}$ (stat), from eq 3 and 4 can be expressed as

$$\Delta G^*_{os,e}(\text{stat}) = \frac{(n + 1 - \alpha)^2 - (n + 1)^2}{n^2 - (n + 1)^2}\Delta G°_{rc,os} - \alpha\Delta G°_{rc,os} \quad (5)$$

Inserting the Born expression for $\Delta G°_{rc,os}$ (eq 2) into eq 5 yields

$$\Delta G°_{os,e}(\text{stat}) = -\alpha(1 - \alpha)(Ne^2/2r\epsilon_s) \quad (6)$$

Interestingly, neither the reactant nor product charges appear in eq 6 so that the same intrinsic barrier would be expected irrespective of their magnitude or sign. Also note that $\Delta G^*_{os,e}(\text{stat})$ is predicted from eq 6 to always be negative.

The contribution to $\Delta G^*_{os,e}$ arising from step 2 of the hypothetical charging process above can be derived by noting that an equivalent charging (or discharging) process is involved to step 1 only in the reverse direction and on a much more rapid time scale than for reorganization of nuclear solvent coordinates. Under these conditions the solvent nuclei are fixed so that the dielectric properties are determined solely by internal electronic polarization, leading to the use of the optical dielectric constant, ϵ_{op}, rather than ϵ_s. This "optical" contribution to $\Delta G^*_{os,e}$, $\Delta G^*_{os,e}(\text{op})$, will always increase the activation free energy since it refers to the formation of a nonequilibrium polarization state. The step 2 charging process is denoted by the vertical ST line in Figure 1A,B.

Following the same procedure as that given above for the static component, we find that

$$\Delta G^*_{os,e}(\text{op}) = \alpha(1 - \alpha)(Ne^2/2r\epsilon_{op}) \quad (7)$$

The free-energy profiles resulting from the sum of the contributions from steps 1 and 2, $\Delta G^*_{os,e}(stat) + \Delta G^*_{os,e}(op) = \Delta G^*_{os,e}$, are also shown in Figure 1A,B. The curve OT is generated from a series of two-step charging processes for different values of α (such as the OS'T' route shown in Figure 1A). The curve TR is the corresponding product curve, generated when the ionic charge in step 2 is instantaneously changed to that of the reduced (product) form rather than back to the reactant charge. The electrochemical free-energy–charge dependence of these "reactant" and "product" curves (Figure 1B) have the same slope and intersect for $\alpha = 0.5$. Inserting $\alpha = 0.5$ into eq 6 and 7 and adding them yields an expression for $\Delta G^*_{int,e}$:

$$\Delta G^*_{os,e} = \frac{Ne^2}{8r}\left(\frac{1}{\epsilon_{op}} - \frac{1}{\epsilon_s}\right) \tag{8}$$

This is the dielectric continuum formula for the outer-shell intrinsic barrier for one-electron electrochemical reactions in the absence of reactant–electrode imaging interactions.[4] Including such imaging in terms of the distance, R_e, from the reactant to its image in the metal yields the well-known relation[4,25]

$$\Delta G^*_{os,e} = \frac{Ne^2}{8}\left(\frac{1}{r} - \frac{1}{R_e}\right)\left(\frac{1}{\epsilon_{op}} - \frac{1}{\epsilon_s}\right) \tag{9}$$

The corresponding expression for the intrinsic outer-shell barrier, ΔG^*_{os}, for homogeneous self-exchange reactions

$$Ox + Red \rightleftharpoons Red + Ox \tag{10}$$
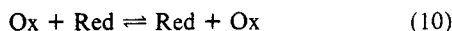
easily follows given that reaction 10 can be viewed as pair of coupled electrochemical reactions (1), yielding twice the overall intrinsic barrier.[24] Taking into account the decrease in solvent polarization resulting from the finite distance between the homogeneous reaction centers, R_h, yields the familiar expression[4] for the homogeneous outer-shell intrinsic barrier:

$$\Delta G^*_{os} = \frac{Ne^2}{4}\left(\frac{1}{r} - \frac{1}{R_h}\right)\left(\frac{1}{\epsilon_{op}} - \frac{1}{\epsilon_s}\right) \tag{11}$$

Incorporating Noncontinuum Factors

Although the foregoing is concerned only with electron transfer within the framework of the conventional dielectric continuum model, the discussion leading to eq 8, 9, and 11 suggests a simple means of generalizing the analysis to include noncontinuum factors. It is evident that the static component of the intrinsic solvent barrier, $\Delta G^*_{os,e}(stat)$, is linked closely to the Born estimate of $\Delta G^°_{rc,os}$ (eq 2) and particularly to the accompanying quadratic dependence of free energy upon ionic charge. Given the well-known severe deficiencies of the Born model for estimating the energetics of ion solvation, it seems preferable to employ instead estimates of $\Delta G^°_{rc,os}$ derived from more sophisticated models, or best of all, from experimental thermodynamic data. All that is necessary is to establish the magnitude of $\Delta G^°_{rc,os}$ and its functional dependence upon ionic charge. To the extent that such parameters are interpretable in terms of specific molecular interactions, the influence of such interactions upon the intrinsic outer-shell barrier can thereby be predicted.

For the sake of simplicity, we will first assume that the component of the outer-shell free energy arising from noncontinuum factors also depends quadratically upon the net ionic charge (vide infra). Figure 2 contains schematic $G^°_{os}$–Z curves designed to illustrate the influence of such specific reactant–solvent interactions upon $\Delta G^*_{os,e}(stat)$ for a cationic redox couple (i.e., where $n \geq 0$). Figure 2A represents the schematic $G^°_{os}$–Z curve expected on the basis of eq 3. Note that the oxidized state, having the higher ionic charge $(n + 1)$, has a more positive outer-shell free energy than the reduced state. This follows on the basis of the continuum model from the imperfect screening of the ionic charge by the surrounding dielectric for finite values of ϵ_s.[26]

Figure 2B represents a schematic $G^°_{os}$–Z curve anticipated as a consequence of charge-dependent specific reactant–solvent in-
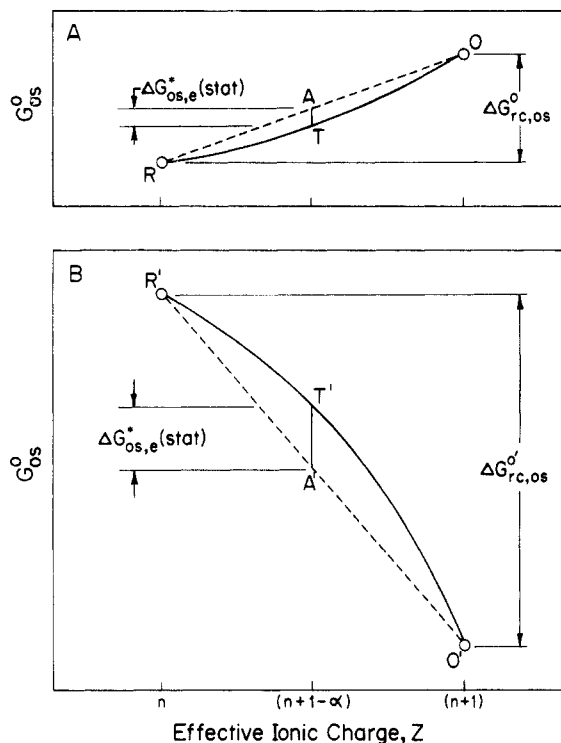
Figure 2. Schematic outer-shell free energy–reaction coordinate plots outlining influence of specific reactant–solvent interactions upon "static" component of outer-shell barrier. (A) Profile expected from the continuum model (eq 3). (B) Profile anticipated in presence of specfic reactant–solvent interactions, with stronger interactions for oxidized (O) relative to reduced (R) species.

teractions. In contrast to Figure 2A, the outer-shell free energy of Ox is now depicted to lie *below* that for Red. This is expected since the greater ionic charge of Ox will engender stronger reactant–solvent interactions, leading to a lower free energy than that for Red. Providing that this additional noncontinuum component of the outer-shell free energy change, $\Delta G^°{}'_{rc,os}$, is quadratically (or at least nonlinearly) dependent upon the ionic charge, then the "bowing" of the $G^°{}'_{os}$–Z curve (O'T'R') shown in Figure 2B will always yield a *positive* component of $\Delta G^*_{os,e}(stat)$, contrasting the *negative* continuum term (eq 6). As for the continuum case, the noncontinuum component of $\Delta G^*_{os,e}(stat)$ will equal the vertical difference (A'T') between the solid bowed curve and the dashed straight line between Ox and Red at the appropriate value of α, as indicated in Figure 2B. Clearly, the magnitude of $\Delta G^*_{os,e}(stat)$ will increase as $\Delta G^°{}'_{rc,os}$ increases.

Generally, then, we may write

$$\Delta G^*_{os,e}(stat) = f[\Delta G^°_{rc,os}(cont)] + f(\Delta G^°{}'_{rc,os}) \tag{12}$$

where the first and second terms on the right-hand side are suitable functions of the solvational energy changes associated with the continuum and noncontinuum components, respectively, of $\Delta G^*_{os,e}(stat)$. Assuming that the former is given by eq 6 and the latter has the same form as in eq 5, if $\alpha = 0.5$ we can write

$$\Delta G^*_{os,e}(stat) =$$
$$\frac{Ne^2}{8r\epsilon_s} + \left[\frac{(n + 0.5)^2 - (n + 1)^2}{n^2 - (n + 1)^2} - 0.5\right]\Delta G^°{}'_{rc,os} =$$
$$-Ne^2/8r\epsilon_s + \Delta G^°{}'_{rc,os}/(8n + 4) \tag{13}$$

If the optical component, $\Delta G^*_{os,e}(op)$, (eq 7) is included along with imaging interactions as before (vide infra), a more general expression for the outer-shell intrinsic barrer results.

$$\Delta G^*_{os,e} = \frac{Ne^2}{8}\left(\frac{1}{r} - \frac{1}{R_e}\right)\left(\frac{1}{\epsilon_{op}} - \frac{1}{\epsilon_s}\right) + \Delta G^°{}'_{rc,os}/(8n + 4) \tag{14}$$

The imaging correction is omitted from the noncontinuum term since the likely short-range nature of the latter should make it insensitive to the proximity of the image charge.

As for the continuum treatment above, eq 14 can be adapted to yield the corresponding relation for the outer-shell intrinsic barrier for homogeneous reactions:

$$\Delta G^{*}_{os} = \frac{Ne^2}{4}\left(\frac{1}{r} - \frac{1}{R_h}\right)\left(\frac{1}{\epsilon_{op}} - \frac{1}{\epsilon_{s}}\right) + \Delta G^{\circ}{}'_{rc,os}/(4n + 2)$$

(15)

Equations 14 and 15 have a similar form to those derived from a corresponding treatment for the intrinsic activation entropy, ΔS^{*}_{int} (eq 14 of ref 24). They provide a simple means of correcting the static portion of the intrinsic solvent barrier for the likely severe deficiencies of the Born model.

Experimental Estimates of $\Delta G^{\circ}{}'_{rc}$

The estimation of outer-shell intrinsic barriers using eq 14 and 15 clearly depends upon the acquisition of at least approximate estimates of the noncontinuum term $\Delta G^{\circ}{}'_{rc,os}$. Since this quantity is a difference in free energy for ions of different charges, values cannot be obtained without resort to some extrathermodynamic assumption. The entropic component of this free-energy difference between Red and Ox (the "reaction entropy") ΔS°_{rc} can be determined reliably from the temperature dependence of the formal potential, E_f, by using a nonisothermal cell arrangement.[20] This is because the temperature dependence of E_f under these conditions approximates closely to the quantity $(d\phi^{\circ}_m/dT)$ required to evaluate ΔS°_{rc}).

The evaluation of $\Delta G^{\circ}_{rc,os}$ values is less straightforward because *absolute* Galvani potentials, rather than their temperature derivatives, are required (eq 4). Nevertheless, *relative* values of $\Delta G^{\circ}{}'_{rc,os}$ for different solvents, $\Delta(\Delta G^{\circ}{}'_{rc,os})$, can be obtained approximately from the corresponding difference in formal potential, $-F(E_f' - E_f'')$.[22] This requires that the formal potentials be evaluated, or estimated, with respect to a reference electrode having a solvent-independent Galvani potential. Although an extrathermodynamic assumption is necessarily involved, such potential scales can be established in different solvents by using, for example, the "tetraphenylarsonium tetraphenylborate" (TATB) assumption. This enables approximate values of $\Delta(\Delta G^{\circ}{}'_{rc,os})$ to be determined from formal potential data.[22]

Although such an approach does not yield the required absolute values of $\Delta G^{\circ}{}'_{rc,os}$, approximate estimates can nonetheless be obtained using a related procedure. This involves plotting E_f for the redox couple of interest on a suitable reference scale in a series of solvents against an empirical solvent parameter that provides a measure of the anticipated reactant–solvent interactions. Providing that a reasonable correlation is obtained, absolute estimates of $\Delta G^{\circ}{}'_{rc,os}$ in a given solvent can be obtained from the difference between E_f in that solvent and the value measured in (or extrapolated to) a solvent environment where such specific interactions are essentially absent.

Redox couples containing ammine and related ligands, such as $Ru(NH_3)_6^{3+/2+}$ and $Co(en)_3^{3+/2+}$ (en = ethylenediamine), are systems with which to illustrate this procedure. These couples have been shown to engage in strong solvent–ligand donor–acceptor interactions with the ammine hydrogen acting as electron acceptors.[22,28] These interactions are stronger in the oxidized state due to the larger positive charge on the ammine hydrogens, leading to increasingly negative values of E_f, and hence larger values of $\Delta G^{\circ}{}'_{rc,os}$, as the donating properties of the solvent increase.[22] A plot of the formal potential for $Ru(NH_3)_6^{3+/2+}$ with respect to that for the ferrocinium–ferrocene (Fc^+/Fc) couple, E_f^{Fc}, in a number of solvents against the solvent "donor number", DN, is given in Figure 3 (line 4). These data were taken from ref 22. The Fc^+/Fc couple provides a suitable "reference reaction" with
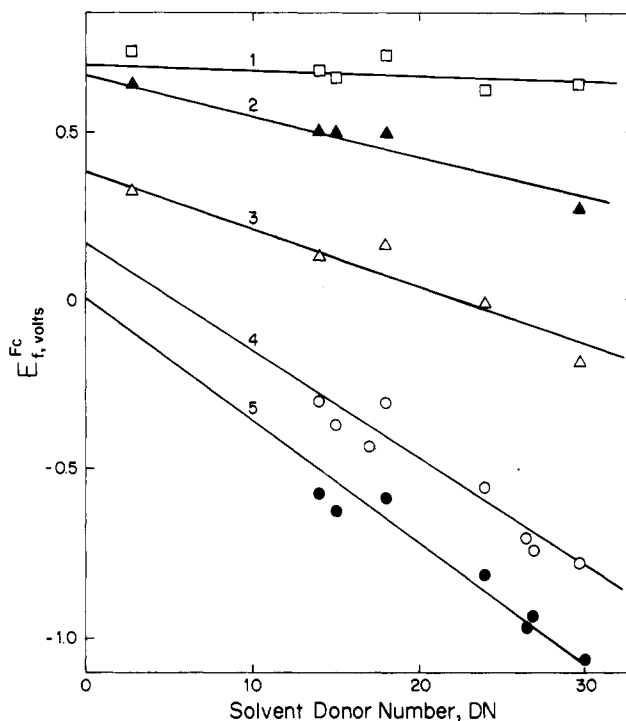
Figure 3. "Donor Selectivity" plots of formal potential of redox couple vs. ferrocinium–ferrocene in given solvent, E_f^{Fc}, against solvent donor number, DN. DN values taken from: Gutmann, V. "Donor-Acceptor Approach to Molecular Interactions"; Plenum Press: New York, 1978; Chapter 2. (1) $Fe(bpy)_3^{3+/2+}$ (bpy = 2,2′-bipyridine); (2) $Ru(NH_3)_2(bpy)_3^{3+/2+}$; (3) $Ru(NH_3)_4bpy^{3+/2+}$; (4) $Ru(NH_3)_6^{3+/2+}$; (5) $Co(en)_3^{3+/2+}$ (en = ethylenediamine). Data for (1), (4), and (5) taken from ref 22; for (2) and (3), from Hupp, J. T., unpublished experiments. Solvents used, in order of increasing donor number (DN values in parentheses): nitromethane (2.7), acetonitrile (14.1), propylene carbonate (15.1), water (18), formamide (24), N,N-dimethylformamide (26.6), N-methylformamide (27), dimethyl sulfoxide (29.8).

which to examine the solvent dependence of E_f associated with ligand acceptor properties. Thus although the electrode potential of this couple does exhibit a mild solvent dependence on the TATB scale,[22] this arises predominantly from an entropic component[29] which evidently is associated with disruption of the internal solvent structure.[23] The intercept of this plot, i.e., the value of E_f^{Fc} where DN = 0, should correspond to the absence of ligand–solvent donor interactions. Thus approximately

$$\Delta G^{\circ}{}'_{rc,os} = -F[E_f^{Fc} - E_f^{Fc}(DN= 0)]$$

(16)

This relationship yields values of $\Delta G^{\circ}{}'_{rc,os}$ for $Ru(NH_3)_6^{3+/2+}$, and similarly for other ammine and related couples[22] that are substantially larger than the Born values obtained from eq 2 in solvents that exhibit moderate or strong electron-donating capability. Besides $Ru(NH_3)_6^{3+/2+}$, representative data for $Co(en)_3^{3+/2+}$ (en = ethylenediamine) are also plotted in Figure 3 (line 5). From Figure 3, $\Delta G^{\circ}{}'_{rc,os} \approx 13$ kcal mol^{-1} for $Ru(NH_3)_6^{3+/2+}$ in water (DN = 18), whereas from the continuum model (eq 2, $\Delta G^{\circ}_{rc,os} = -3.0$ kcal mol^{-1} for $r = 3.5$ Å.[22] Insertion of $\Delta G^{\circ}{}'_{rc,os} = 13$ kcal mol^{-1} into eq 15, given that $n = 2$ for $Ru(NH_3)_6^{3+/2+}$, yields $\Delta G^{*}_{os} = 7.8$ kcal mol^{-1} for $r = 3.5$ Å and $R_h = 7$ Å. The conventional continuum treatment (eq 11) yields $\Delta G^{*}_{os} = 6.5$ kcal mol^{-1}. The additional noncontinuum term in eq 15 therefore constitutes a small yet significant (1.3 kcal mol^{-1}) component of ΔG^{*}_{os}.

For comparison, Figure 3 (line 1) shows corresponding data for $Fe(bpy)_3^{3+/2+}$ (bpy = 2,2′-bipyridine), again taken from ref 22. This system is an example of a couple that engages in relatively nonspecific ligand–solvent interactions since coordinated 2,2′-bipyridine does not contain any polar groups anticipated to interact specifically with the surrounding solvent. As expected the E_f^{Fc}–DN

(28) Mayer, U.; Kotocova, A.; Gutmann, V.; Gerger, W. *J. Electroanal. Chem.* **1979**, *100*, 875. Kotocova, A.; Mayer, U. *Collect. Czech. Chem. Commun.* **1980**, *45*, 335.

(29) Sahami, S.; Weaver, M. J. *J. Solution Chem.* **1981**, *10*, 199.

plot has a slope close to zero, so that $\Delta G^{\circ}_{rc,os} \sim 0$ even in strongly donating solvents such as dimethyl sulfoxide and N,N-dimethylformamide. The same behavior is also seen for other polypyridine couples, such as $Ru(bpy)_3^{3+/2+}$, $Cr(bpy)_3^{3+/2+}$, $Co(bpy)_3^{3+/2+}$, and $Fe(phen)_3^{3+/2+}$ (phen = 1,10-phenanthroline).[22] Noncontinuum factors are therefore unlikely to contribute significantly to the intrinsic outer-shell barrier for these couples. Plots of E_f^{Fc} against solvent DN for two mixed ammine–bipyridine couples, cis-$Ru(NH_3)_2(bpy)_2^{3+/2+}$ and $Ru(NH_3)_4bpy^{3+/2+}$, are also shown in Figure 3 (lines 2 and 3).[22] Note that the slopes of these plots are intermediate between those for $Fe(bpy)_3^{3+/2+}$ and $Ru(NH_3)_6^{3+/2+}$. Indeed the E_f^{Fc}–DN slopes (the "solvent donor selectivity") are approximately proportional to the number of ammine ligands, suggesting that each ligand provides an independent additive contribution to the overall solute–solvent interactions.

Several other types of noncontinuum contributions to the static component of ΔG^*_{os} may also be anticipated. Thus reactants containing donating groups, such as complexes having chiefly anionic ligands and radical anions with electronegative centers, may interact specifically with solvents which can act as strong electron acceptors. For example a correlation, analogous to that in Figure 3, has been observed between the formal potential for $Fe(CN)_6^{3-/4-}$ and the electron-accepting ability of the solvent as measured by the "acceptor number".[30]

It is important to recognize that such specific reactant–solvent interactions are only anticipated to influence the reaction energetics when the extent of such interactions differ between Ox and Red. The forms of eq 14 and 15 indicate that the influence of these specific interactions will always *increase* the intrinsic barrier provided that they are greater for the redox state carrying the larger net charge. The applicability of these relations is also dependent on the occurrence of a quadratic relation between the free energy and the net ionic charge (vide infra).

Comparisons with Experiment

The inclusion of noncontinuum contributions to the outer-shell intrinsic barrier as in eq 14 and 15 provide corrections to the conventional treatment that can at least qualitatively account for some of the apparent discrepancies seen with solvent-dependent kinetic data.[12–15] However, a difficulty of testing such theoretical predictions with rate data is that a number of factors besides the outer-shell barrier can dominate the observed solvent dependence, such as uncertainties in work term corrections,[15,18] nonadiabaticity, and solvent dynamical effects upon the preexponential factor.[16] Further examination of this matter will be considered elsewhere.

A more direct test of models for the solvent intrinsic barrier is provided by solvent-dependent studies of photoinduced electron transfer within symmetrical binuclear complexes in homogeneous solution. This is because the reorganization energy is directly probed via the intervalence spectral transition energy rather than indirectly via reaction rates.[31b]

The intramolecular electron-transfer system $[(NH_3)_5Ru^{III}$-$(4,4'-py)Ru^{II}(NH_3)_5]^{5+}$ studied in several solvents by Creutz[31a] is particularly germane to the present discussion since significant noncontinuum contributions to ΔG^*_{os} arising from ammine ligand–solvent interactions would be expected on the basis of eq 15.

Table I contains a comparison between the experimental and theoretical intrinsic barriers for this system in five solvents of varying donicity. The experimental outer-shell barriers, ΔG^*_{os}-(expt), were obtained from the experimental optical reorganization energies, λ_{expt}, by subtracting the inner-shell component calculated

TABLE I: Noncontinuum Contributions to Optical Electron-Transfer Barrier for $(NH_3)_5Ru^{III}(4,4'-bpy)Ru^{II}(NH_3)_5$

solvent	ΔG^*_{os}(expt)[a] (1)	ΔG^*_{os}(cont)[b] (2)	ΔG^*_{os}-(eq 15)[c] (3)	(1) – (2)	(1) – (3)
D_2O	6.80	6.65	7.77	0.15	-0.97
CH_3OH	6.46	6.46	7.52	0	-1.06
CH_3CN	6.33	6.36	7.30	-0.03	-0.97
DMF	6.13	5.71	7.36	0.42	-1.23
Me_2SO	5.78	5.45	7.30	0.33	-1.52

[a] Intrinsic outer-shell barrier (kcal mol^{-1}) for reaction in solvent listed, extracted from optical absorption data in ref 31a as outlined in the text. [b] Intrinsic outer-shell barrier (kcal mol^{-1}) as estimated from dielectric continuum model (eq 11) with $r = 4.0$ Å, $R_h = 8.0$ Å (see ref 31a). [c] Intrinsic outer-shell barrier (kcal mol^{-1}) as estimated from eq 15. Continuum component calculated as in footnote b; values of $\Delta G^{\circ\prime}_{rs,os}$ for noncontinuum term estimated from data in Figure 3 by using eq 16 as noted in text.

from structural data to yield the outer-shell component, λ_{os}, and noting that $\Delta G^*_{os} = \lambda_{os}/4$.[31] The continuum estimates, ΔG^*_{os} (cont), were obtained by taking $r = 4.0$ Å and $R_h = 8$ Å in eq 11 as noted in ref 31a. The corresponding noncontinuum-corrected estimates, ΔG^*_{os} eq 15, were obtained by evaluating the additional noncontinuum term in eq 15. The appropriate values of $\Delta G^{\circ}_{rc,os}$ were obtained from eq 16 by assuming that the plot of E_f^{Fc} vs. DN for the $Ru(NH_3)_5^{3+/2+}$ moiety is 25 mV per DN unit (estimated by interpolation from the data for the $Ru(NH_3)_4bpy^{3+/2+}$ and $Ru(NH_3)_6^{3+/2+}$ couples in Figure 3).

The last two columns in Table I report the differences between the values of ΔG^*_{os}(expt) and the corresponding theoretical quantities derived from the continuum and noncontinuum-corrected treatments. As anticipated from eq 15, the former (eq 11) does slightly underestimate the magnitude of ΔG^*_{os}(expt) for solvents of higher DN (e.g., DMF, Me_2SO). However, the noncontinuum component in eq 16 apparently *overestimates* this correction by ca. 3–5 fold, so that ΔG^*_{os}(expt) < ΔG^*_{os}(eq 15). The simple continuum treatment therefore yields values of ΔG^*_{os} that are numerically closer to ΔG^*_{os}(expt) than are those obtained with inclusion of the noncontinuum component. This result might be taken as evidence against the validity of the noncontinuum correction itself. It is more likely, however, that the close correspondence between ΔG^*_{os}(expt) and ΔG^*_{os}(cont) is somewhat fortuitous, especially given the uncertainties as to the exact applicability of the simple "two-sphere" model embodied in both eq 11 and 15 to systems of differing geometries.[4b] Thus several modifications to eq 11 that take into account interactions between the reacting cospheres yield somewhat (10–30%) smaller values of ΔG^*_{os}(cont). Inclusion of the additional noncontinuum component as in eq 15 to such relations yields estimates of ΔG^*_{os} that are closer to ΔG^*_{os}(expt) than are obtained in its absence.

Discussion

The foregoing demonstrates that short-range reactant–solvent interactions can constitute only a small ($\lesssim 1$–2 kcal mol^{-1}) component of the outer-shell intrinsic barrier even in the face of a large or even predominant influence of such factors upon the redox thermodynamics. Moreover, the data in Table I suggest that the noncontinuum effect may be even smaller than that expected from eq 14 and 15.

The quantitative validity of these relations rests primarily on the correctness of the assumed quadratic dependence of $\Delta G^{\circ}_{rc,os}$ upon the net ionic charge. The quadratic dependence of the continuum portion, $\Delta G^{\circ}_{rc,os}$, assumed in deriving these relations, is predicted from a statistical–mechanical treatment based on ion–solvent and solvent–solvent multipole interactions.[34,35] However, this seems less likely to be entirely correct for the noncontinuum component, $\Delta G^{\circ\prime}_{rc,os}$, associated with specific ligand–solvent interactions. These can be viewed as individual

(30) Gutmann, V.; Gritzner, G.; Danksagmuller, K. *Inorg. Chim. Acta* **1976**, *17*, 81. Gritzner, G.; Danksagmuller, K.; Gutmann, V. *J. Electroanal. Chem.* **1978**, *90*, 203.

(31) (a) Creutz, C. *Inorg. Chem.* **1978**, *17*, 3723. (b) Cruetz, C. *Prog. Inorg. Chem.* **1983**, *30*, 1.

(32) A similar slope, 22 mV per DN unit, is obtained for $Ru(NH_3)_5^{3+/2+}$ from published data[33] for the asymmetric binuclear complex $[(NH)_5Ru(py)RuCl(bpy)_2]^{4+}$; this supports the validity of applying "donor selectivity" data obtained for mononuclear redox couples to such binuclear systems.

(33) Powers, M. J.; Callahan, R. W.; Salmon, D. J.; Meyer, T. J. *Inorg. Chem.* **1976**, *15*, 1457.

(34) Friedman, H. L.; Krishnan, C. V. In "Water—A Comprehensive Treatise"; Franks, F., Ed.; Plenum Press: New York, 1973; Vol. 3, pp 39–42.

(35) Golden, S.; Guttman, C. *J. Chem. Phys.* **1965**, *43*, 1894.

charge–dipole interactions, the charge residing on the ligand acceptor (or donor) site and varying with the oxidation state. Such charge–dipole interactions vary *linearly* with the charge,[36] the quadratic component for ion–solvent interactions being associated instead with the mutual interaction of dipoles between solvent molecules.[34] Moreover, variations in the central ionic charge are anticipated to yield proportionately smaller changes in the effective charge on the ligands[37] thereby providing more linear variations of $\Delta G^{\circ\prime}_{rc,os}$ with ionic charge. Unfortunately, no direct experimental information is available. Some support to this expectation is nevertheless provided by the very similar variations in E_f^{Fc} observed for $Ru(NH_3)_6^{3+/2+}$ and $Ru(NH_3)_5NCS^{2+/+}$ with solvent DN.[23,39] Therefore $\Delta G^{\circ\prime}_{rc,os}$ might be expected to vary with charge in a manner intermediate between linear and quadratic. Since the noncontinuum contribution to ΔG^*_{os} will entirely disappear in the former case, one might expect that eq 14 and 15, obtained by assuming the latter case, provide *upper limits* to the magnitude of this effect.

It is therefore concluded that even extensive changes in short-range reactant–solvent interactions may yield only small and even negligible influences upon the outer-shell intrinsic barrier. This is not to say that such interactions do not strongly affect the reaction energetics but rather that this influence is largely accounted for by the driving force component of the free-energy barrier so that is has little effect upon the intrinsic portion. It is important to note that contemporary electron-transfer theories are largely concerned with calculating ΔG^*_{int} and the *dependence* of the activation barrier upon the driving force. The reaction thermodynamics, upon which the primary influence of solvent noncontinuum factors are felt, are not addressed by these theories, their evaluation being left entirely to experiment.

Other Limitations of the Continuum Treatment

It is also of importance to examine if the validity of the continuum component of eq 14 and 15, contained in the first term on the right-hand side of these relationships, is itself liable to be influence by short-range reactant–solvent interactions. It might be anticipated that smaller values of ϵ_s than the normal bulk values would be appropriate in eq 14 and 15, especially for multicharged ions, due to partial dielectric saturation in the vicinity of the reactant. Although small effective values of ϵ_s are deduced for solvent molecules in the primary solvation shell, values that approach that for the bulk medium are estimated for the secondary and subsequent shells,[40] i.e., the "outer shell" considered here. In any case, since typically $\epsilon_{op} \gtrsim 20\epsilon_s$ this static component should yield only a relatively small ($\lesssim 5\%$) contribution to ΔG^*_{os}. Especially small effective values of ϵ_s in the outer shell might be anticipated for reactants that strongly orient surrounding solvent molecules by means of specific donor–acceptor interactions. However, since this effect is predicted to decrease ΔG^*_{os} (eq 15), it should tend to be offset by the small corresponding increase in ΔG^*_{os} anticipated from the noncontinuum term.

It remains to consider possible noncontinuum effects upon the optical component of ΔG^*_{os}, as expressed in eq 7. Since ϵ_{op} is typically small (ca. 1.5–2) the optical component commonly provides a large, probably predominant, contribution to ΔG^*_{os}. Similarly to ϵ_s, the appropriate value of ϵ_{op} to use in eq 14 and 15 is an appropriately weighted "local" quantity representative of nearby solvent molecules. This might be anticipated to differ from the bulk ϵ_{op} value, at least with reactants featuring extensive short-range solvent polarization. However, ϵ_{op} is expected to be insensitive to the intermolecular solvent structure since it reflects only the electronic polarizability of the solvent molecules.

Moreover, the relatively small ϵ_{op} values indicate that the "screening" ability of the nonequilibrium polarization by surrounding solvent molecules is relatively ineffective; this polarization should therefore extend over relatively large distances from the reactant center where ϵ_{op} should closely approximate the average bulk value. At least for water molecules, the anisotropy of the electronic polarizability (and hence of ϵ_{op}) is small[41] so that even extensive short-range solvent orientation should have little influence on the effective value of ϵ_{op} in eq 14 and 15. Nevertheless, significant variations in ϵ_{op} in the vicinity of solutes can be anticipated for more asymmetric solvents, especially those that are strongly oriented by the reactant.

In a recent polemical article, Khan and Bockris[42] have suggested another possible source of noncontinuum effects for strongly hydrated ions associated with "inner-shell"-like distortions of water molecules in the secondary solvation shell. Such a contribution can be considered in terms of the average alteration in hydrogen-bond distances between the coordination shell of aquo (or possibly other hydrogen-bonding) ligands and adjacent water molecules brought about by electron transfer. The magnitude of this contribution to ΔG^*_{int}, ΔG^*_{os} (O⋯H), can in principle be determined from the conventional expression[1e]

$$\Delta G^*_{int} = 0.5nf_i(\Delta a/2)^2 \qquad (17)$$

where Δa is the equilibrium bond-distance change brought about by electron transfer, f_i is the reduced force constant of the ith bond, and n is the number of bonds undergoing distortion. A rough estimate of Δa for $M(OH_2)_6^{3+/2+}$ couples is provided by the ca. 0.1-Å difference in the O⋯H hydrogen bond distance between primary and secondary hydration for M^{3+} vs. M^{2+} crystalline hydrates.[43] A force constant of ca. 3×10^4 dyn cm is estimated for such hydrogen bonds from spectral data,[44] which for $n = 6$, yields $\Delta G^*_{os}(O⋯H) \sim 1$ kcal mol^{-1}. Although only a very rough estimate, this demonstrates that such distortions of secondary shell solvation may provide a significant additional contribution to ΔG^*_{int} for strongly hydrogen-bonded systems. Such a contribution may account in part for the surprisingly large solvent deuterium isotope effects observed for both electrochemical and homogeneous exchange of metal aquo complexes.[46-48] Thus the slighly stronger hydrogen-bonding properties anticipated for the deuterated ligands[49] may yield a larger average value of n and hence of ΔG^*_{os} (O⋯H) in eq 17.

This "microscopic" approach to estimating components of ΔG^*_{os} associated with specific reactant–solvent interactions is quite distinct from, yet complementary to, the phenomenological approach embodied in eq 14 and 15. It is important to recognize that such vibrational distortion, similarly to the "optical" component of the hypothetical two-step charging process, will contribute to ΔG^*_{os} *irrespective* of the functional form of the free energy–reaction coordinate profile associated with these processes. In contrast, the "static" component of ΔG^*_{os} is associated only with the nonlinear portion of the free-energy charging curve for this process. This is because the former describe components of

(36) Bockris, J. O'M.; Reddy, A. K. N. "Modern Electrochemistry"; Plenum Press: New York, 1970; Vol. I, Chapter 2.

(37) In harmony with this expectation, fractional changes in the charge residing on the aquo hydrogens are calculated to be induced when $Fe(OH_2)_6^{3+}$ is reduced to $Fe(OH_2)_6^{2+}$.[38]

(38) Jafri, J. A.; Logan, J.; Newton, M. D. *Isr. J. Chem.* 1980, *19*, 340.

(39) Sahami, S. Ph.D. Thesis, Michigan State University, 1981.

(40) Hasted, J. B. "Aqueous Dielectrics"; Chapman and Hall: London, 1973; Chapter 5.

(41) Kern, C. W.; Karplus, M. In "Water—A Comprehensive Treatise"; Franks, F., Ed.; Plenum Press: New York, 1972; Vol. 1, Chapter 5.

(42) Khan, S. U. M.; Bockris, J. O'M. In "Chemistry and Physics of Electrocatalysis"; McIntyre, J. D. E., Weaver, M. J., Yeager, E., Eds.; Electrochemical Society: Pennington, NJ, 1984.

(43) From data compilation in: Falk, M.; Knop, O. In "Water—A Comprehensive Treatise"; Franks, F., Ed.; Plenum Press: New York, 1973; Vol. 2, Chapter 2.

(44) Obtained from vibrational frequency, 160–190 cm^{-1}, of hydrogen bonds in liquid water[45] by assuming a reduced mass equal to that for a single water molecule.

(45) Walrafen, G. E. In "Water—A Comprehensive Treatise"; Franks, F., Ed.; Plenum Press: New York, 1972; Vol. 1, Chapter 5.

(46) Weaver, M. J.; Tyma, P. D.; Nettles, S. M. *J. Electroanal. Chem.* 1980, *114*, 53.

(47) Weaver, M. J.; Li, T. T.-T. *J. Phys. Chem.* 1983, *87*, 1153.

(48) Weaver, M. J.; Nettles, S. M. *Inorg. Chem.* 1980, *19*, 1641.

(49) Arnett, E. M.; McKelvey, D. R. "Solute-Solvent Interactions"; Coetzee, J. F.; Ritchie, C. D., Eds.; Marcel Dekker: New York, 1967; Chapter 6.

ΔG^*_{os} associated with *nonequilibrium* solvent polarization which are necessarily absent in the reactant and product states.

Concluding Remarks

Along with the related examination of specific reactant–solvent effects upon the intrinsic entropic barrier,[24] the present phenomenological treatment further demonstrates the virtues of employing electrochemical thermodynamic data to yield insight into the role of reactant–solvent interactions upon the kinetics of electron-transfer reactions. The results indicate that such interactions may typically yield only a surprisingly small contribution to the intrinsic barrier. The well-documented severe limitations of the Born and other continuum models for estimating the thermodynamics of ionic solvation[34,36] are demonstrated to exert

surprisingly little influence upon the solvation component of the intrinsic barrier. Nevertheless, noncontinuum effects may contribute more significantly to ΔG^*_{os} for systems that involve vibrational distortions of outer-shell solvent molecules. Especially in this regard, the formulation of molecularly based theoretical models for the outer-shell reorganization process[50] should be most revealing.

(50) Calef, D. F.; Wolynes, P. G. *J. Chem. Phys.* **1983**, *78*, 470.

Interpretation of the Fluorescence Decay of 1-Methylindole in Polar Solvents by Reorientational Effects

I. Gonzalo*

Departamento de Optica y Estructura de la Materia, Facultad de C. Físicas, Universidad Complutense, 28040 Madrid, Spain

and T. Montoro

Laboratoire de Photophysique Moleculaire du C.N.R.S., Bat. 213, Université de Paris-Sud, 91405 Orsay Cedex, France (Received: August 14, 1984; In Final Form: November 19, 1984)

The fluorescence decay curves of 1-methylindole in butanol at different temperatures have been interpreted, taking into account the reorientation of the solute–solvent dipole moments as a time-dependent phenomenon during fluorescence. Thus, the reorientation times have been estimated and observed to vary rapidly between room temperature and 155 K. The anomalous decay can be interpreted as a competition between fluorescence and reorientation. These results are in agreement with those deduced from a previous study of fluorescence spectral shifts.

Introduction

This study concerns polar molecules whose dipole moments $\bar{\mu}$ change through electronic excitation. The indolic molecules are a biophysically interesting class of molecules whose dipole moments undergo a significant increase ($|\Delta\bar{\mu}| \simeq 2.4$ D[1–4]). This includes a noticeable change of direction in $\bar{\mu}$, approximately 48°. When these molecules are dissolved in polar solvents, this change is manifested by shifts in the maxima of the fluorescence spectra, varying with temperature and viscosity. These shifts are a consequence of different solute–solvent relaxation energies,[5–7] owing to the relative reorientation of the solute–solvent dipole moments. The influence of solvent viscosity and temperature on the reorientation dynamics has been studied with laser techniques for DODCI in alcohols.[8]

If the viscosity of the solvent is high or the temperature is low, the very slow reorientation under these circumstances causes the solute molecule to fluoresce from an excited state that is not yet in equilibrium with the surrounding solvent. The time dependence of the shifts has been taken into account in some treatments.[8–10]

A time-dependent solute–solvent interaction was calculated by Bagchi et al.,[9] considering a frequency-dependent dielectric continuum for the solvent. In that work, the assumption was made that solute molecules have no specific interactions with the surrounding solvent and that the solute does not become much more polar under excitation.

In this paper an interpretation is made of the fluorescence decay time curves at different temperatures for 1-methylindole in butanol in the framework of the model proposed in a previous work[10] to account for the fluorescence spectral shifts.

Since 1-methylindole cannot form hydrogen bonds, it was preferred to indole which forms such bonds. So, we should be able to see more distinctly the reorientational relaxation at different temperatures in 1-methylindole than in indole.

The method consists in the evaluation for a given temperature of a statistical group of solute molecules, each one having a different stabilization energy depending on the local average kinetic energy of the surrounding solvent molecules.[10]

A theoretical decay function is established here and it has been fitted to the experimental decay curves. In this way, the electronic excited-state lifetimes and reorientation lifetimes could be estimated at different temperatures. There is a competition between fluorescence and reorientation. Therefore, decay curves portray fluorescence decays from reoriented, nonreorientated, and partially reorientated excited states. The obtained results imply that the solvent reorientation time should be equal to the solute fluorescence time at a temperature close to 211 K. This agrees with what has been derived from the interpretation of the spectral shifts.[10] The

(1) A. Kawski and G. Karcz-Jacyno, *Bull. Acad. Pol. Sci.*, **21**, 289 (1973).
(2) A. Kawski and J. Sepiol, *Bull. Acad. Pol. Sci.*, **20**, 737 (1972).
(3) A. Kawski and I. Gryczynski, *Bull. Acad. Sci.*, **21**, 1061 (1973).
(4) L. F. Gladchenko and L. G. Pikulik, *Zh. Prik. Spectrosk.*, **6**, 355 (1967).
(5) A. López-Campillo and T. Montoro, *C. R. Acad. Sci. Paris, Ser. B*, **29**, 271 (1981).
(6) Ken-Ichi Itoh and Tohrn Azumi, *J. Chem. Phys.*, **62**, 3431 (1975).
(7) E. Lippert, W. Luder, and F. Moll, *Spectrochem. Acta*, **10**, 858 (1959).
(8) D. H. Waldeck and G. R. Fleming, *J. Phys. Chem.*, **85**, 2614 (1981).
(9) B. Bagchi, D. W. Oxtoby, and G. R. Fleming, *Chem. Phys.*, **86**, 257 (1984).

(10) I. Gonzalo and J. L. Escudero, *J. Phys. Chem.*, **86**, 2896 (1982).